

# Crystallization and melting behaviour of photodegraded polypropylene – II. Re-crystallization of degraded molecules

M. S. Rabello† and J. R. White\*

Materials Division, Department of MMME, University of Newcastle upon Tyne  
Newcastle upon Tyne NE1 7RU UK

(Received 12 July 1996; revised 4 December 1996)

Isotactic polypropylene bars were exposed to ultraviolet radiation (UV) in the laboratory for periods up to 48 weeks causing a reduction in molecular size and the build-up of chemical groups like carbonyls and hydroperoxides. The specimens were re-crystallized from the melt under isothermal and non-isothermal conditions and investigations were conducted by differential scanning calorimetry (DSC), X-ray diffraction, and light microscopy. At first the fractional crystallinity of the re-crystallized materials increased with exposure as the result of decreasing molecular size, but for longer exposures the fractional crystallinity decreased because of the increase in concentration of chemical impurities. In highly degraded specimens, the presence of  $\gamma$ -phase crystals was detected. Kinetic studies revealed that the rates of nucleation and growth may be affected differently by photodegradation, and that the degraded molecules crystallized much faster than the unexposed material when their rates of crystallization under the same supercooling are compared. Double melting peaks were observed in DSC thermograms and were shown to be due to re-organization during heating, but in some cases the segregation of highly defective molecules is the major reason for peak doubling. Molecular segregation also changes the spherulite morphology during crystallization, as revealed by polarized light microscopy. © 1997 Elsevier Science Ltd.

(Keywords: polypropylene; photodegradation; crystallization)

## INTRODUCTION

The chemical structure of molecules in a degraded polymer sample may be substantially different from that present initially because chemical degradation causes several changes in molecules, including chain scission, branching, crosslinking, and the introduction of other chemical groups like carbonyls, hydroperoxides, esters, etc. In the case of polypropylene, the main effects of photo-oxidation are the reduction in molecular size and the formation of extra chemical groups<sup>1</sup>.

The crystallization of (virgin) polypropylene from the melt has attracted much attention and the factors that control the kinetics and the subsequent melting behaviour are fairly well established<sup>2–10</sup>. However, just a few studies were made regarding the kinetics of crystallization and melting behaviour of degraded polypropylene<sup>11–13</sup>, even though this has an inherent importance in the recycling of degraded materials<sup>14</sup>. The crystallization of photo-degraded polypropylene from the melt is expected to depend on the molecular size and on the chemical constitution of the molecules. Since both factors are substantially altered by oxidation, many differences to the unexposed material are expected, but their relative contributions are not easy to predict.

In this work the crystallization behaviour of photo-degraded polypropylene crystallized isothermally and

non-isothermally from the melt is investigated in injection-moulded specimens exposed for up to 48 weeks. Changes in crystal structure and fractional crystallinity were followed by X-ray diffraction, whereas the kinetics of crystallization were studied by differential scanning calorimetry. The crystallization and melting behaviour of degraded polypropylene were correlated with the chemical changes introduced by the photo-oxidation as determined by infrared spectroscopy and gel permeation chromatography. The current paper describes a study of the re-crystallization behaviour of specimens taken from the injection-moulded bars that were the subject of the morphological studies described in Paper 1<sup>15</sup>.

## EXPERIMENTAL

Injection-moulded bars (3.1 mm thick) were produced from a commercial grade of isotactic polypropylene (ICI GXE 35) using a Butler–Smith 100/60 injection moulding machine. The injection pressure was 107 MPa; the barrel and nozzle temperatures were both 200°C, and the mould temperature was 40°C. The bars were exposed to ultraviolet radiation in the laboratory for periods up to 48 weeks according to the procedure described in the preceding paper<sup>15</sup>.

The studies described here were conducted with specimens removed from the exposed surface of the bars to a depth of 0.2 mm. The dependence of molecular weight and carbonyl index on the exposure time is shown in *Figure 1*, obtained by gel permeation chromatography and infrared spectroscopy, as detailed elsewhere<sup>15</sup>.

\* To whom correspondence should be addressed.

† Permanent address: Department of Materials Engineering, Federal University of Paraíba, Av. Aprigio Veloso 882, Campina Grande, PB, Brazil.

The re-crystallization experiments were conducted in a differential scanning calorimeter (DSC). Specimens weighing 5–6 mg were heated to 210°C, and then crystallized under either isothermal or non-isothermal conditions during which thermograms were recorded using a Mettler FP90 controller connected to a FP85 Heat Flux DSC cell. The non-isothermal crystallization was carried out from 210 to 40°C at a constant cooling rate (normally 13°C min<sup>-1</sup>). In isothermal crystallization, the specimens were fast cooled (~100°C min<sup>-1</sup>) to the isothermal crystallization temperature ( $T_c$ ) and kept at  $T_c$  for an extended period. The time allowed for each isothermal crystallization depended on the chosen value of  $T_c$  and on the amount of degradation in the sample (up to 420 min). Following standard procedures<sup>16,17</sup>, Avrami plots were constructed from the crystallization exotherms and the rate of crystallization was determined as the inverse of the time to reach 50% of the maximum crystallinity at a chosen temperature. The equilibrium melting temperature ( $T_m^0$ ) was determined according to the method of Lauritzen and Hoffman<sup>18</sup> by plotting the melting point ( $T_m$ ) for several crystallization temperatures then extrapolating to the line  $T_m = T_c$ . All experiments were conducted under nitrogen flow (50 ml min<sup>-1</sup>) to minimize thermal degradation effects.

Selected experiments were also conducted in a Mettler FP84 cell. This cell can be used for microscopical observations while simultaneously running a DSC scan and was set to operate under the same conditions applied for the normal DSC experiments. A small amount of sample was melted between two cover slips and observed using an Olympus BH-2 light microscope arranged for polarized light transmission microscopy. A sensitive tint plate was inserted between the crossed polars to determine the sign of birefringence. The images were recorded continuously with a video camera and some photographs shown here were taken from a Sony video printer camera in posterior analysis. The spherulite radius was measured from the images for selected times during isothermal crystallization.

Specimens for X-ray diffraction experiments were prepared under controlled conditions in the DSC cell using a larger amount of material (ca. 25 mg). The analyses were conducted with a Phillips PW 1050 diffractometer using Cu K $\alpha$  Ni-filtered radiation (wavelength = 0.154 nm). The fractional crystallinity ( $f_c$ ) was calculated according to the method developed by Weidinger and Hermans<sup>19</sup>, as explained elsewhere<sup>20</sup>.

## RESULTS AND DISCUSSION

### Non-isothermal crystallization

Figure 2 shows the effect of UV exposure on the crystallization temperature of polypropylene (PP), obtained during cooling at 13°C min<sup>-1</sup>. The crystallization temperature, taken as the position of the maximum of the exothermic peak, decreased linearly with exposure time, presumably due to the progressively lower molecular weight and larger number of chemical irregularities present in the molecules of the exposed material (Figure 1). It is well known that shorter and defective molecules crystallize more slowly<sup>3,4</sup>, and this is likely to be true for the case of degraded PP. The observed crystallization temperature reflects the overall rate of crystallization which depends on both the rates of nucleation and growth. The isothermal crystallization studies (described below) indicated that the chemical irregularities and molecular size may affect differently the rates of nucleation and growth.

Figure 3 shows diffractograms for photo-degraded PP crystallized from the melt. In samples exposed for 18 weeks and longer, a reduction of the intensity from (130) planes (centred at  $2\theta \sim 18.5^\circ$ ) and the appearance of a peak at  $2\theta \sim 19.5\text{--}20^\circ$  were observed. It is likely that the peak

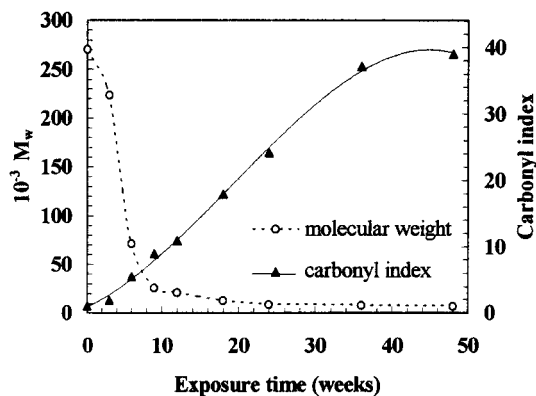


Figure 1 Effect of exposure time on the molecular weight and carbonyl index of PP

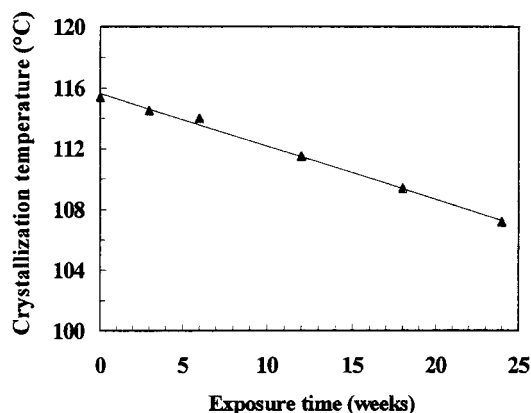


Figure 2 Effect of exposure time on the non-isothermal crystallization temperature

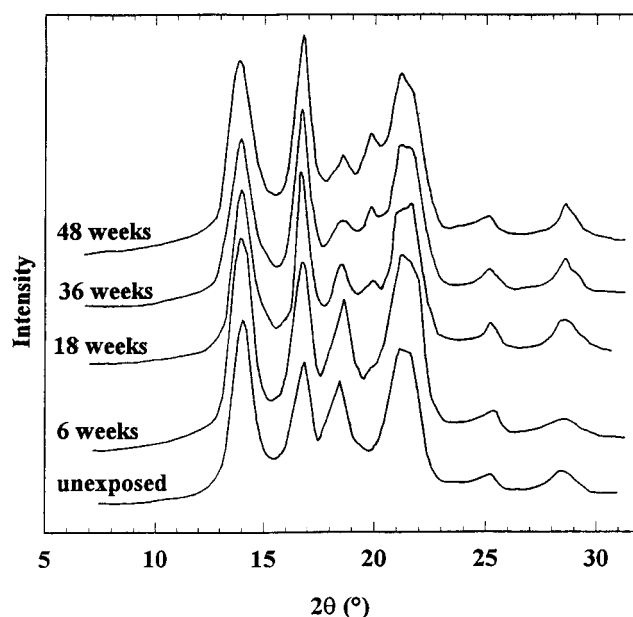


Figure 3 X-ray diffractograms (Cu K $\alpha$ ) of PP samples after UV exposure and re-crystallization at 13°C min<sup>-1</sup>

occurring at 19.5–20° corresponds to the  $\gamma$ -phase, since it is the only crystal phase of polypropylene that shows a strong reflection in this range of  $2\theta$ <sup>21</sup>. The  $\gamma$ -phase of PP was initially assigned a triclinic lattice, but recent studies suggest that it may have an orthorhombic lattice<sup>22,23</sup>. In the past this structure was reported to be observed only in low molecular weight<sup>21</sup>, low tacticity<sup>24</sup> fractions of polypropylene and in random copolymers<sup>25</sup>. More recently, the  $\gamma$ -phase has been obtained with commercial, high molecular weight grades<sup>26</sup>, sometimes under high pressure<sup>22</sup> or under high orientation<sup>27</sup>. It has been shown that the presence of defects favours  $\gamma$ -phase crystallization<sup>28</sup>. In the present investigation, it is apparent that the  $\gamma$ -phase was obtained as a result of the presence of short and defective molecules since it was detected only in highly degraded samples.

The degree of crystallinity data determined from the X-ray diffractograms are given in Figure 4. It increased initially with exposure time and then decreased sharply. This behaviour can be associated with the two main effects of photodegradation: chain scission and build-up of carbonyl and other impurity groups. The reduction in molecular size dominates in short-time exposures and favours crystallization, whereas after longer times the presence of many extraneous groups in the molecules of highly degraded specimens renders crystallization more difficult. The degraded material will always contain a significant fraction of crystallizable polymer in the form of short segments that come from the crystals, which remain undamaged during exposure. The fractional crystallinity of polypropylene is known to increase with reduction in molecular weight<sup>29</sup> and to decrease with reduction in stereoregularity<sup>5</sup>. The molecular structure of the degraded polypropylene analysed here can be compared with PP random copolymers or PP with low tacticity in which the regularity is reduced. The results in Figure 4 seem to be consistent with this idea.

The effect of photodegradation on the melting enthalpy is given in Figure 5. The curve shows essentially the same features as that for the fractional crystallinity obtained by X-ray diffraction, with an initial increase followed by a sharp decrease in property. However, the sensitivity of changes in enthalpy seems to be different to that for X-ray crystallinity. A possible explanation for this discrepancy between the DSC and X-ray results is that the degradation causes a reduction in the melting enthalpy of the pure crystals in re-crystallized samples due to the incorporation of defects into the crystals. This is assumed to be similar to unexposed PP containing atactic sequences, in which the equilibrium melting enthalpy decreases with decreasing regularity of the molecules<sup>5</sup>. A similar anomaly was noted with poly(ether-ether-ketone)<sup>30</sup>, when the melting enthalpy decreased to zero after electron irradiation, but electron microscopy and X-ray experiments revealed that the crystals were almost unaltered by degradation.

#### Kinetics of isothermal crystallization

The results for the rate of isothermal crystallization are shown in Figure 6 for all conditions studied. The crystallization rate of polypropylene is drastically reduced with exposure time, with the exception of the materials weathered for only 3 weeks, which crystallized faster than the virgin polymer at the same temperature. Presumably, the results obtained reflect the effects of chemical degradation on PP (Figure 1): (i) the build-up of chemical irregularities tends to decrease the rate of crystallization, like in PP with

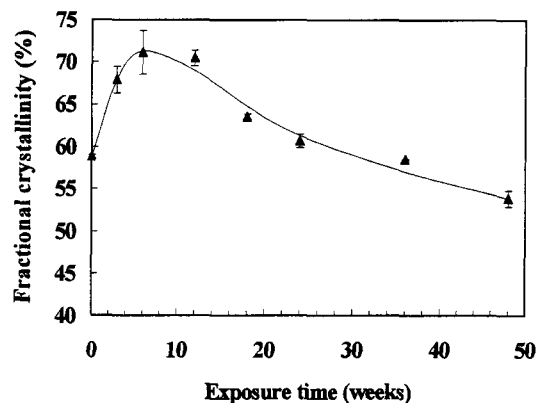


Figure 4 Effect of photodegradation on the fractional crystallinity of PP after non-isothermal crystallization as obtained by X-ray diffraction

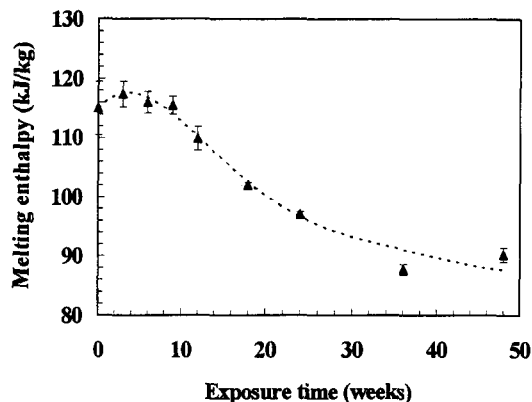


Figure 5 Melting enthalpy of photo-degraded PP crystallized from the melt

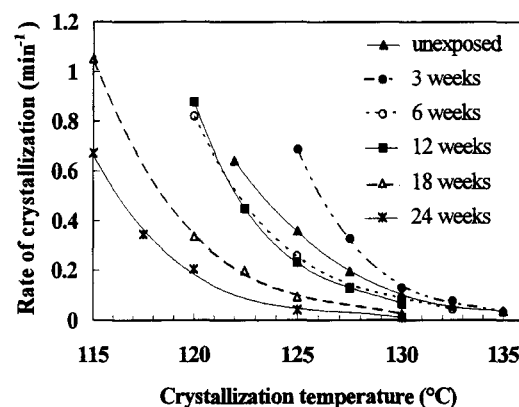


Figure 6 Effect of crystallization temperature on the rate of crystallization of PP exposed for various times

decreasing tacticity<sup>3,4</sup> or containing a co-monomer<sup>6</sup>; (ii) the decrease in molecular weight can decrease or increase the rate of crystallization, depending on the actual value<sup>31</sup>.

The comparison of the rates of crystallization at the same temperature for all samples, however, may not represent a suitable guide to their ability to crystallize. This is because the rate of crystallization of a polymer is strongly dependent on the supercooling, defined as

$$\Delta T = T_m^0 - T_c \quad (1)$$

The equilibrium melting temperature  $T_m^0$  is the upper limit for crystal melting and it is an intrinsic property of the

polymer, virtually uninfluenced by factors like crystal size. Comparisons between several types of samples, such as those suffering different amounts of photodegradation, are best performed when based on the same supercooling rather than on the same crystallization temperature.

In order to normalize the crystallization conditions, the equilibrium melting temperature of the samples was determined. The value of  $T_m^0$  obtained for the unexposed material was 190.8°C, which is within the range commonly reported for isotactic polypropylene<sup>32</sup>, although there is some dispute on the best procedure to determine this property<sup>33</sup>. Figure 7 shows that the equilibrium melting temperature decreased sharply at 6 weeks exposure, followed by a moderate decrease at longer exposures. This is probably a combined effect of reduction in molecular weight and increasing imperfection of crystallites caused by the inclusion in the crystals of impurity chemical groups present on the chains. For exposure beyond 6 weeks, the decrease in  $T_m^0$  was rather small, despite the fact that there was still an increase in the carbonyl index (Figure 1). It may be that there is a limit to the concentration of chemical irregularities that can be fitted into the crystals and that this corresponds to a saturation effect.

Figure 8 shows that when the rate of crystallization is plotted against the supercooling, the trend is markedly different from the one of Figure 6. Now, for the same supercooling, the crystallization is much faster for degraded samples than for the unexposed polypropylene. The crystallization process involves the thermodynamic driving force and kinetic factors. At a constant supercooling, the

thermodynamic driving force for crystallization should be the same for all samples, hence the differences in the kinetics may reflect the inherent crystallizabilities of the molecules. There is not, however, a uniform trend in relation to the time of exposure. The rate increases with time of weathering up to 12 weeks, and then there is a decrease beyond that time, with the sample exposed for 6 weeks showing a similar behaviour to the one exposed for 24 weeks. This can result from the combined effects of several factors that control crystallization:

- (1) reduction in molecular weight increases the crystallizability
- (2) increase in polarity increases the crystallizability
- (3) chemical irregularities decrease the crystallizability

The kinetics of crystallization depend on the relative importance of the nucleation and growth rates. These rates may be changed differently by the oxidation effects, namely molecular weight and carbonyl index (Figure 1). For the same supercooling, the decrease in molecular weight tends to increase the spherulite growth rate<sup>34</sup> whereas the increase in chemical irregularities within the molecules decreases the rate of growth<sup>4</sup>. The rate of nucleation on the other hand is affected mainly by the presence of extra chemical groups; a slight increase in polarity increases the rate of nucleation<sup>11</sup> and a high concentration of chemical irregularities reduces it<sup>35</sup>. Therefore, factors 1 and 2 above seem to be predominant for low exposure time, whereas for longer exposures the chain impurities begin to control the kinetics of crystallization. The large shift to the left-hand side of the curves in Figure 8 for the samples exposed for 6 weeks and

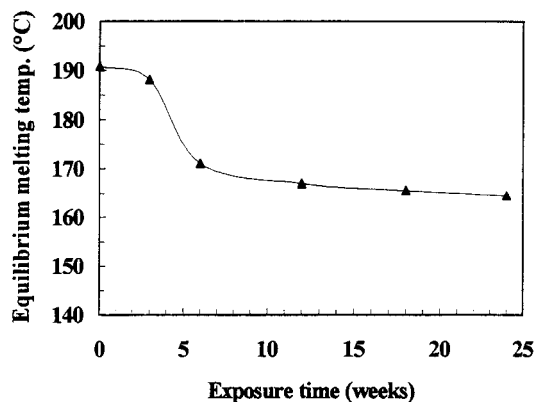


Figure 7 Effect of exposure time on the equilibrium melting temperature

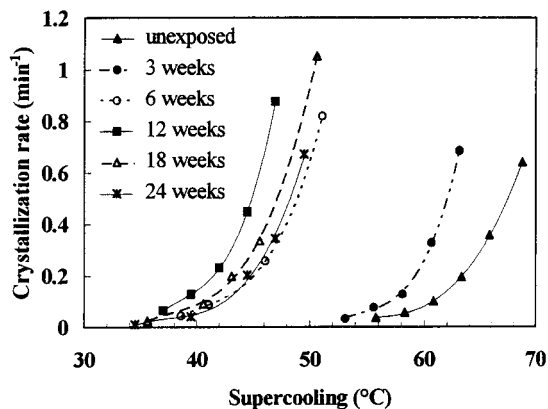


Figure 8 Effect of supercooling on the rate of crystallization of PP exposed for various times

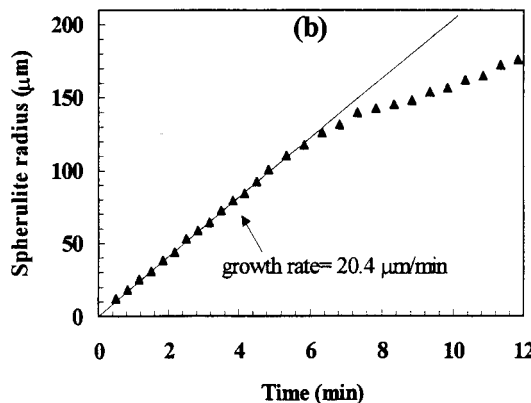
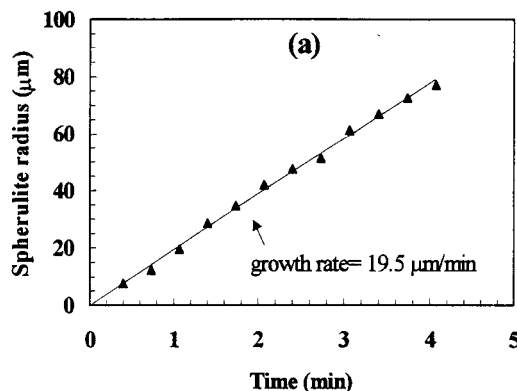


Figure 9 Spherulite radius during isothermal crystallization at 125°C for (a) unexposed and (b) 6 weeks exposed polypropylene. The deviation from linearity in the later stages of crystallization for the 6 weeks exposed sample is discussed in the section ‘‘Avrami analysis’’

longer may be due to the drastic reduction in molecular weight which could increase the molecular mobility, and, as a consequence, the growth rate.

In support of the hypothesis offered above that the rate of growth and nucleation are influenced differently by the effects of degradation, an example is given in *Figure 9* showing the increase of spherulite radius during isothermal crystallization at 125°C of unexposed and 6 weeks exposed PP. At the same  $T_c$ , the supercooling is much lower for the exposed specimen and, nevertheless, it showed a growth rate slightly higher than the unexposed one ( $20.4 \mu\text{m min}^{-1}$  c.f.  $19.5 \mu\text{m min}^{-1}$ ). The rate of nucleation was lower for the exposed material, however, as can be seen from the number of spherulites in *Figure 10*.

#### Avrami analysis

Avrami plots for unexposed and selected degraded samples are shown in *Figure 11*. The Avrami exponent  $n$  was close to 2 for the majority of samples and conditions investigated, with no strong effect of temperature or extent of photodegradation. This value for  $n$  is in agreement with several other studies on polypropylene within a similar range of temperatures<sup>5,7,10</sup>, and it corresponds to a disc-like morphology formed by heterogeneous nucleation<sup>16,7</sup>.

The plots for virgin polypropylene featured only one straight line, whereas the exposed material showed two straight lines, indicating that crystallization was a two-stage process, namely primary (stage I) and secondary (stage II) crystallization.

It is well known that the second stage of crystallization in polymers results from spherulite impingement at the latter

stages of the primary crystallization, decreasing the crystallization rate<sup>31</sup>. The secondary crystallization then takes place in the intraspherulitic region<sup>36</sup> which, due to steric reasons and the competition between the impinging spherulite, is much slower than the primary crystallization. According to this interpretation, the second stage does not change the size of spherulite; hence it is not detected visually by light microscopy. It has been argued that the rate of the secondary crystallization is lower than that of the primary crystallization because it follows after the segregation of low molecular weight molecules, which, at a fixed crystallization temperature, are at a lower supercooling than the high molecular weight fractions<sup>7</sup>.

It follows from the argument of the previous paragraph that virgin PP should display a two-stage Avrami plot since it has a relatively broad distribution of molecular weights ( $M_w/M_n = 8$ ). It is possible that the limited sensitivity of the DSC cell has not detected the expected secondary crystallization in this sample<sup>16</sup>.

The degraded polymer displayed a two-stage process and the reasons why it is observed will now be considered. Firstly, it is important to bear in mind that the photo-degraded polypropylene consists of a mixture of a number of different molecular species, with different chemical defect contents and different molecular sizes. The reasons for the existence of this mixture are: (i) the random nature of the chemical degradation; (ii) different rates of degradation in the amorphous and crystalline regions; (iii) different extents of degradation through the thickness direction of the layer (0.2 mm thick) removed for the analysis. This will be reflected in the kinetics of crystallization because of

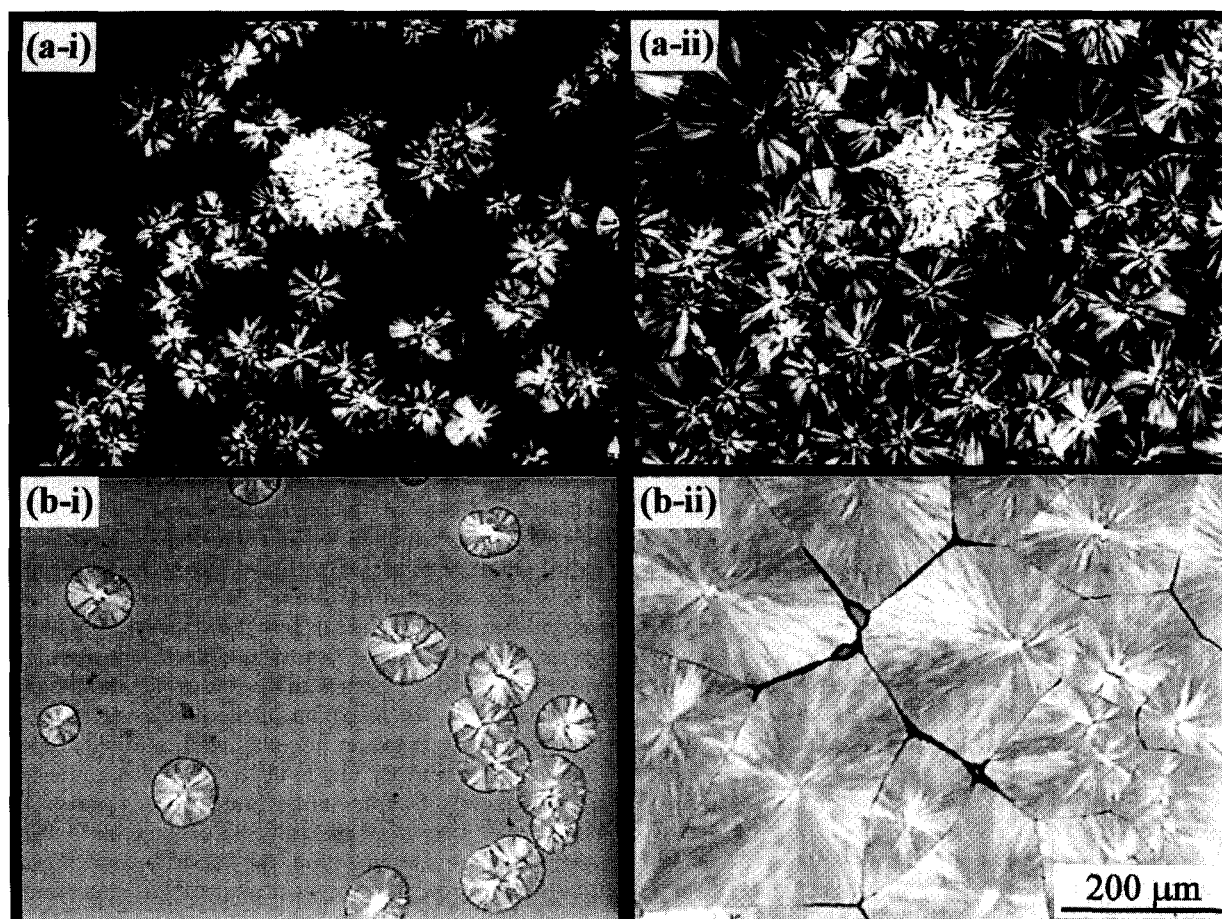


**Figure 10** Spherulitic morphology of (a) unexposed PP and (b) 6 weeks exposed PP during crystallization at 125°C: (i) at 2 minutes; (ii) at the end of crystallization

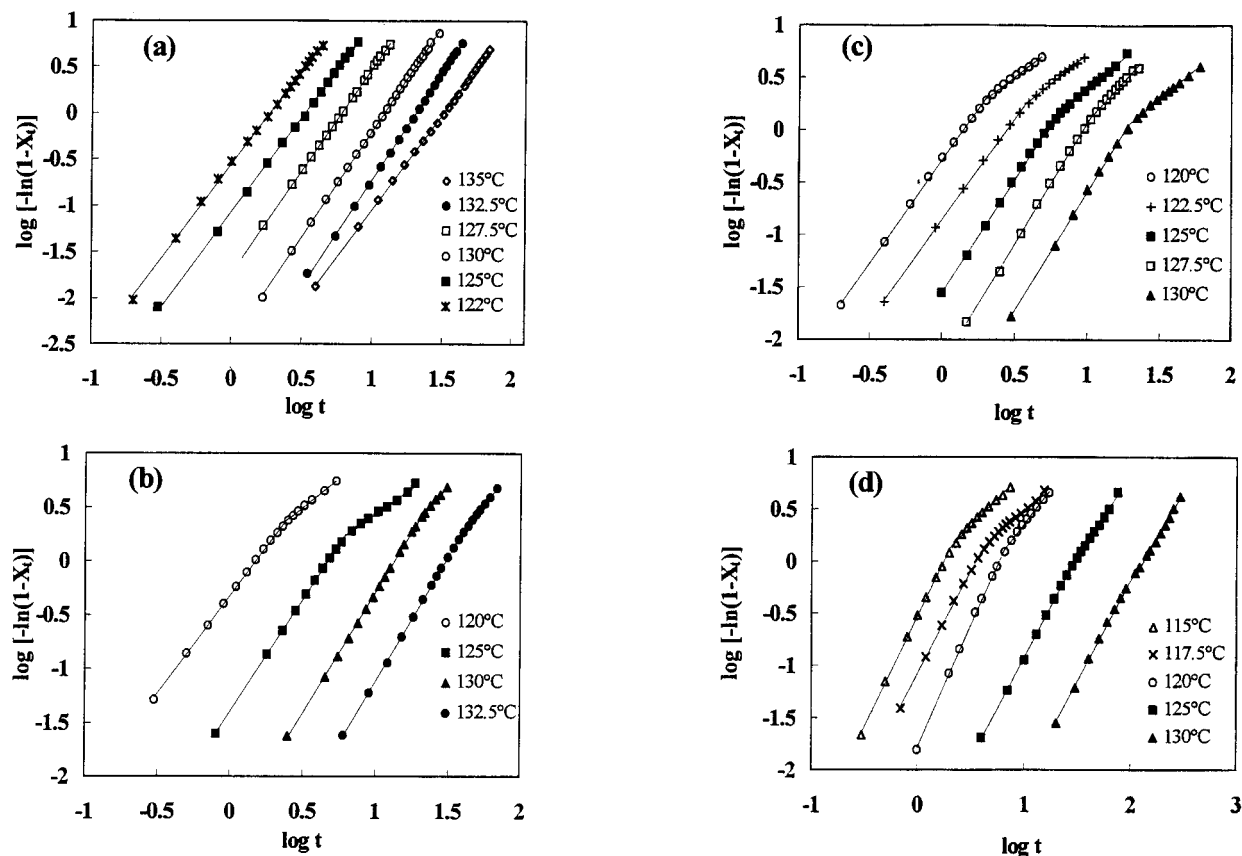


**Figure 11** Avrami plots for (a) unexposed PP and for PP exposed for (b) 6 weeks, (c) 12 weeks, and (d) 24 weeks.  $X_t$  is the relative crystallinity at a time  $t$ , obtained from the crystallization exotherms

molecular segregation effects. The less defective molecules crystallize faster and the more defective (and smaller) ones may be rejected by the growing crystals to crystallize later, after spherulite impingement<sup>37</sup>. A larger concentration of defective molecules is present in degraded PP in comparison with the unexposed polymer, and can be expected to enhance the secondary crystallization step, rendering the two-stage process observable. This is rather similar to what was observed with low tacticity PP<sup>3</sup>.

The results shown in *Figure 9b* also highlight another aspect of the crystallization of degraded PP, which is that a decrease in growth rate was observed before the spherulite impingement had occurred. Interestingly, the time when the growth rate changed ( $\sim 7$  min) in *Figure 9b* corresponds to the time when the break occurred in the Avrami plot of *Figure 11b* (which was based on DSC data). A similar type of correlation was observed with other samples and conditions. It is possible, therefore, that the two-stage crystallization shown in the Avrami plots in degraded PP is not due to the onset of secondary crystallization in the interlamellar region, but corresponds instead to a change in spherulite growth rate. The decrease in growth rate is likely to be caused by the presence of more defective molecules that were rejected by the growing crystals in the early stages of crystallization. These molecules are less crystallizable (or not crystallizable at all) and they can diffuse to the spherulite boundaries, decreasing the rate of crystallization. The remaining molecules can then crystallize at the later stages of spherulite growth or during the secondary crystallization stage. A decrease in growth rate during isothermal crystallization of mixtures of isotactic and atactic polypropylene was observed by Keith and Padden<sup>34</sup>. They suggested that this happens when the diffusion rate of

impurities (the atactic molecules) is higher than the growth rate of the spherulites and that the defective molecules accumulate at the surface of the growing spherulites.

#### Morphological characteristics

From *Figure 10b*, it is apparent that no change in morphology was associated with the transition in growth rate. An experiment carried out at  $T_c = 120^\circ\text{C}$  with a 24 weeks exposed material, however, revealed that a transition in morphology can take place during isothermal crystallization (*Figure 12*). It is clear that from the very beginning of crystallization, the spherulite of this material grew with 'serrated' boundaries in contrast to the smooth growth front obtained with the unexposed specimens shown in *Figure 10a*. The 6 weeks exposed PP also gave spherulites which grew with a serrated front (*Figure 10b*) but the serrations were of smaller amplitude. This type of morphology occurs due to the enhanced fibrillation caused by the presence of impurities at the spherulite periphery<sup>38,39</sup>. It was suggested that fibrillation arises from random surface instabilities at the growing front of spherulite, which may result in layers formed from less defective molecules that have higher growth rates than the rest of the interface<sup>40</sup>. The consequence is the break up of the planar interface into a 'fibrous' habit between regions with a higher impurity content. The fibrillar appearance of spherulites does not mean that they are necessarily formed from fibrous crystals, but, instead, consist of an aggregate of lamellae<sup>41</sup>. With the progression of crystallization, the impurity concentration in the remaining melt increases considerably<sup>34</sup> and there is an intensification of the spherulite fibrillation. This is evident from *Figure 12c-d*. The final morphology shown in *Figure 12* features spherulites with distinct characteristics: a

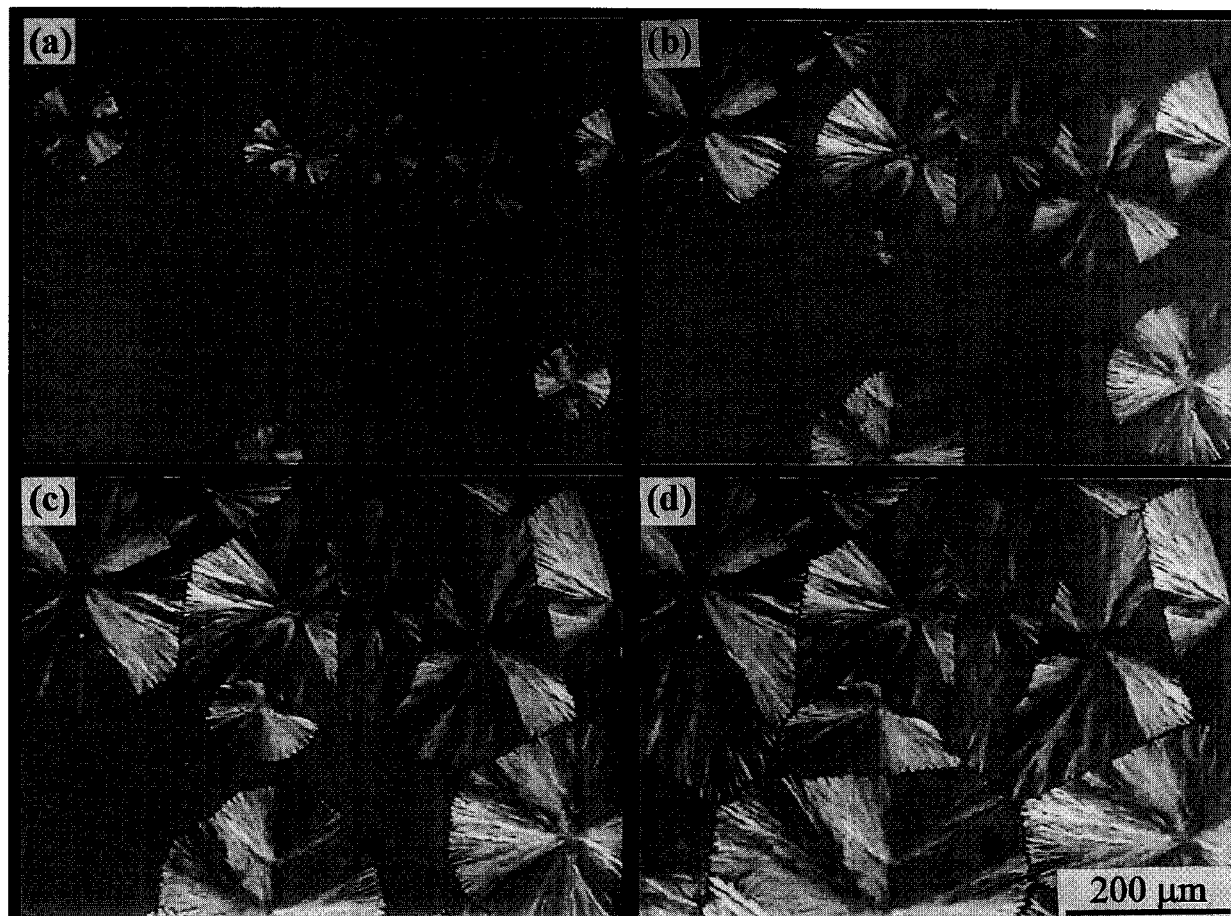


**Figure 12** Growing spherulites at 120°C in a PP sample exposed for 24 weeks: (a) 2.5 minutes; (b) 5 minutes; (c) 7 minutes; (d) end of crystallization

'normal' texture in the middle and a fibrillar character towards the periphery. It is also apparent that the spherulites did not really impinge at the end of crystallization, a fact that may be attributed to the location at the interspherulitic boundaries of segregated non-crystallizable molecules.

According to the theory of polymer crystallization proposed by Keith and Padden<sup>38,40</sup>, the texture of polymer spherulites may be defined by the parameter  $\delta = D/G$ , where  $D$  is the diffusion coefficient of impurities and  $G$  is the growth rate. This parameter represents the thickness of a layer rich in impurities next to the advancing front and determines the lateral dimensions of the crystals. The higher the value of  $\delta$ , the coarser the texture because the impurities tend to concentrate at the boundaries of the growing spherulites. Although the parameter  $\delta$  was shown to be quantitatively inaccurate to represent the crystal dimensions<sup>41</sup>, this approach could be invoked to differentiate (in a qualitative way) the morphologies displayed in *Figure 10b* and *Figure 12*. In comparison with the unexposed PP, the highly degraded samples have higher impurity diffusion rates (due to the lower molecular weight of the defective molecules) and possibly lower growth rates (due to the presence of more chemical irregularities). Therefore, the thickness of the impurity-rich layer  $\delta$  is expected to be larger in the degraded PP, which is consistent with a coarser and more open texture shown in *Figure 12*. However, the texture also depends on the crystallization temperature. With decreasing  $T_c$ , an increase in  $G$  and a decrease in  $D$  are expected, resulting in lower values of  $\delta$  because the defective molecules tend to be entrapped within the intra-spherulitic regions. Accordingly, *Figure 13* shows that the

final morphology of a 24 weeks exposed sample crystallized at 115°C featured uniform spherulites and the 'serrated' texture is not as evident as in *Figure 12d*. The segregation of impurities has also occurred in the sample shown in *Figure 13*, evidenced by the gaps between spherulites.

#### *Melting behaviour of non-isothermally crystallized samples*

During the DSC heating of non-isothermally crystallized PP, double endotherms were obtained for samples exposed for 6 weeks and longer (*Figure 14*), with a peak or shoulder situated on the high temperature side of the thermograms. The intensity of the subsidiary peak was higher for the 6- and 9-weeks exposed materials and decreased for longer exposure times.

There are numerous reports of the occurrence of double endotherms during DSC experiments on virgin isotactic polypropylene. Many explanations have been offered, including the presence of different crystal structures and/or morphologies<sup>42,43</sup>; crystal transformation during heating<sup>44,45</sup>; reorganisation during heating<sup>5,46</sup>; and segregation of molecules with low molecular weight or with irregularities that form crystals with lower  $T_m$ <sup>47,48</sup>. In the study of degraded PP, although there are several reports of peak doubling<sup>49–52</sup>, there are very few attempts to offer suitable interpretations. Since there are substantial changes in the molecular structure in degraded PP, the reasons for the DSC peak doubling may not be necessarily the same as in the undegraded polymer.

In the current work, it is speculated that the double melting peaks may be due to one of the following reasons: (i) melting of crystals with different melting points; or (ii)

re-crystallization or re-organization during heating. The presence of  $\gamma$ -phase may be related to double peaks only in highly degraded samples where this phase was detected and therefore will not be considered as a major contributor to the double endotherms.

The first hypothesis (hypothesis (i)) considers that the molecular segregation (evidenced in the previous section) also occurs during non-isothermal crystallization and results in the formation of two different populations of crystals that melt in different temperature ranges, like in many polymer blends<sup>53</sup>.

The second hypothesis (hypothesis (ii)) considers that phase segregation during non-isothermal crystallization does not occur to a significant extent (because of the fast crystallization conditions), leaving the less crystallizable species entrapped within the spherulites<sup>39</sup> and, therefore, molecule segregation is not the major contributor to the double peaks. The proposal is that degraded molecules form relatively unstable crystals during rapid cooling and that on re-heating they melt then re-crystallize into a more stable phase that subsequently melts at a higher temperature, leading to a double peak in the DSC thermogram. After long exposure times, the ability to form the second, more stable, phase during the DSC experiment is reduced because of increased defect content, hence double peaks would become less evident after prolonged exposures.

In an attempt to elucidate the reason for the double melting peaks, an experiment was conducted, which consisted of partial melting of the material (6 weeks exposed sample) at a temperature between the two endotherms (chosen as 158°C). The specimen was initially prepared by melting then crystallizing by cooling at 13°C min<sup>-1</sup> to 90°C. The sample was then heated at 6°C min<sup>-1</sup> to 158°C and kept for 5 minutes at this temperature, then cooled at 13°C min<sup>-1</sup>, and finally heated at 6°C min<sup>-1</sup> for the DSC analysis. If hypothesis (i) is true, then the thermal treatment at 158°C would melt the low  $T_m$  crystals, and these molecules would crystallize again during cooling from 158°C. On subsequent heating, both peaks would reappear. If hypothesis (ii) is correct, then the time spent at 158°C would lead to transformation of the low temperature phase into the high temperature phase, and only single peaks would be obtained on the final heating. The thermogram obtained during the final melting is displayed in Figure 15 in comparison with the original one. It contains a strong peak in the high melting temperature region and only a hint of an endotherm in the low melting temperature region. This experiment suggests that re-crystallization during the DSC run is the explanation for the double endotherms observed with samples non-isothermally crystallized from the melt. Experiments similar to those used to obtain Figure 15 were carried out with PP exposed for 12 and 24 weeks, again choosing dwell temperatures between the DSC peaks obtained on the first heating. Comparable observations were obtained<sup>54</sup>.

To eliminate possible effects of self-seeding after partial melting that would otherwise alter the melting temperature of the crystals, a final experiment was conducted on a sample crystallized at 13°C min<sup>-1</sup>. This consisted of a fast heating (~100°C min<sup>-1</sup>) to 158°C, followed by immediate heating from 158°C at 6°C min<sup>-1</sup>. If hypothesis (ii) is correct, then no peak would be observed in the thermogram recorded in the final stage (above 158°C) since insufficient time was given for the formation of the high temperature phase. This was indeed what happened, as shown in Figure 16.

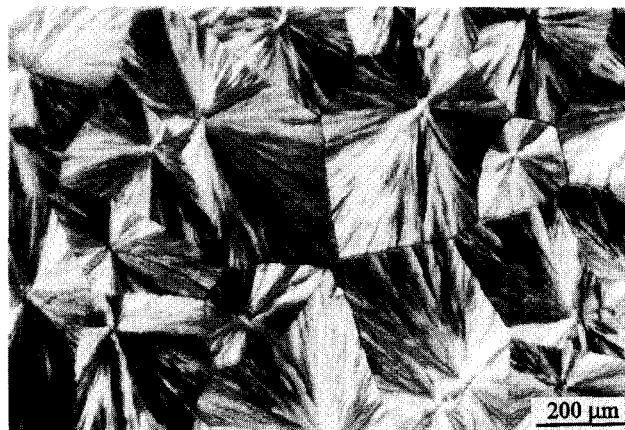


Figure 13 Final morphology of 24 weeks exposed PP crystallized at 115°C

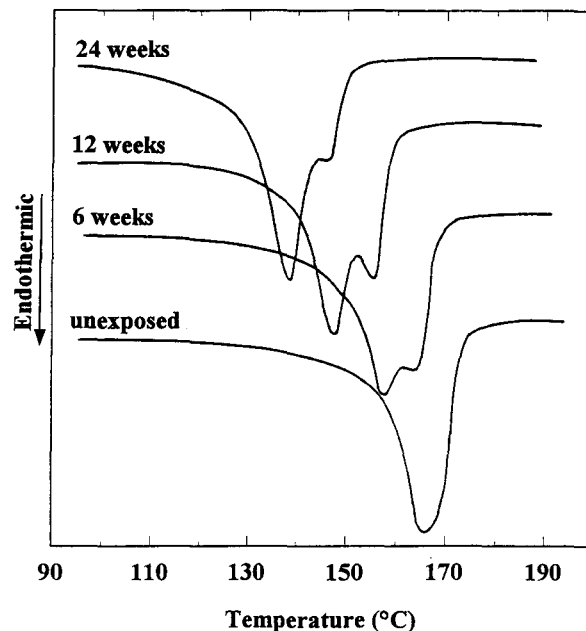


Figure 14 Melting thermograms of PP after various exposure times. Scanning rate = 6°C min<sup>-1</sup>

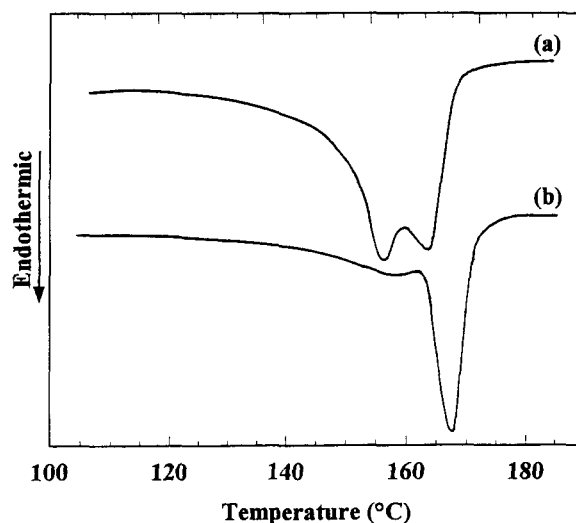


Figure 15 Melting thermograms of PP exposed for 6 weeks. (a) Original trace obtained by cooling at 13°C min<sup>-1</sup> then heating at 6°C min<sup>-1</sup>; (b) after partial melting at 158°C



The re-organization during heating was clearly observed by polarized light microscopy. A specimen of PP that had been UV-exposed for 6 weeks then crystallized from the melt at  $13^{\circ}\text{C min}^{-1}$  featured 'mixed' spherulites (Figure 17a) according to the classification of Padden and Keith<sup>55</sup>. When the spherulites were heated, the regions of positive birefringence changed to negative just before the temperature of partial melting was reached (Figure 17b). The change in birefringence of PP during heating has been suggested to be due to melting of tangential lamellae, that are normally thinner than the radial ones, resulting in a

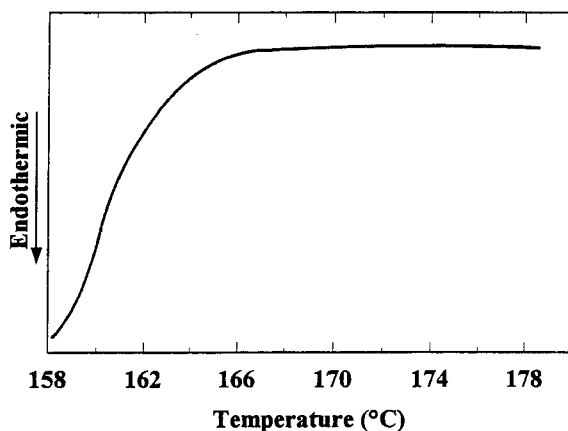


Figure 16 DSC trace for a 6 weeks exposed PP heated rapidly to  $158^{\circ}\text{C}$  then heated at  $6^{\circ}\text{C min}^{-1}$

higher concentration of radial lamellae which give the negative birefringence character<sup>56</sup>. When the temperature approached  $158^{\circ}\text{C}$ , there was a significant decrease in birefringence, resembling a melting stage (Figure 17c), and after some time at this temperature the spherulites reappeared in the same positions, with a stronger negative birefringence (Figure 17d). The changes occurred slowly with no indication that a rapid martensitic-type solid state transformation was involved. From the images recorded it is not clear whether the morphological changes in Figure 17 involved a true melting stage or that it was a solid–solid transformation with an intermediate stage with reduced birefringence. The spherulite obtained in Figure 17d melted in the range of temperature corresponding to the main melting peak of Figure 15b.

#### Melting behaviour of isothermally crystallized samples

The melting thermograms for the unexposed and exposed PP after isothermal crystallization displayed either a single peak or a main peak accompanied by a shoulder on the low temperature side. The latter occurred only with specimens crystallized at high temperatures and an example is shown in Figure 18 for a sample exposed for 6 weeks. This type of melting behaviour is consistent with what is commonly reported in the literature, in which double peaks are observed in virgin PP only when the sample is crystallized at low (ca.  $T_c < 120^{\circ}\text{C}$ ) or at high (ca.  $T_c > 130^{\circ}\text{C}$ ) temperatures<sup>6,57</sup>. The peak duplication of virgin PP crystallized at high temperatures was suggested to be due to the presence of distinct crystal populations<sup>5,42</sup>, which is

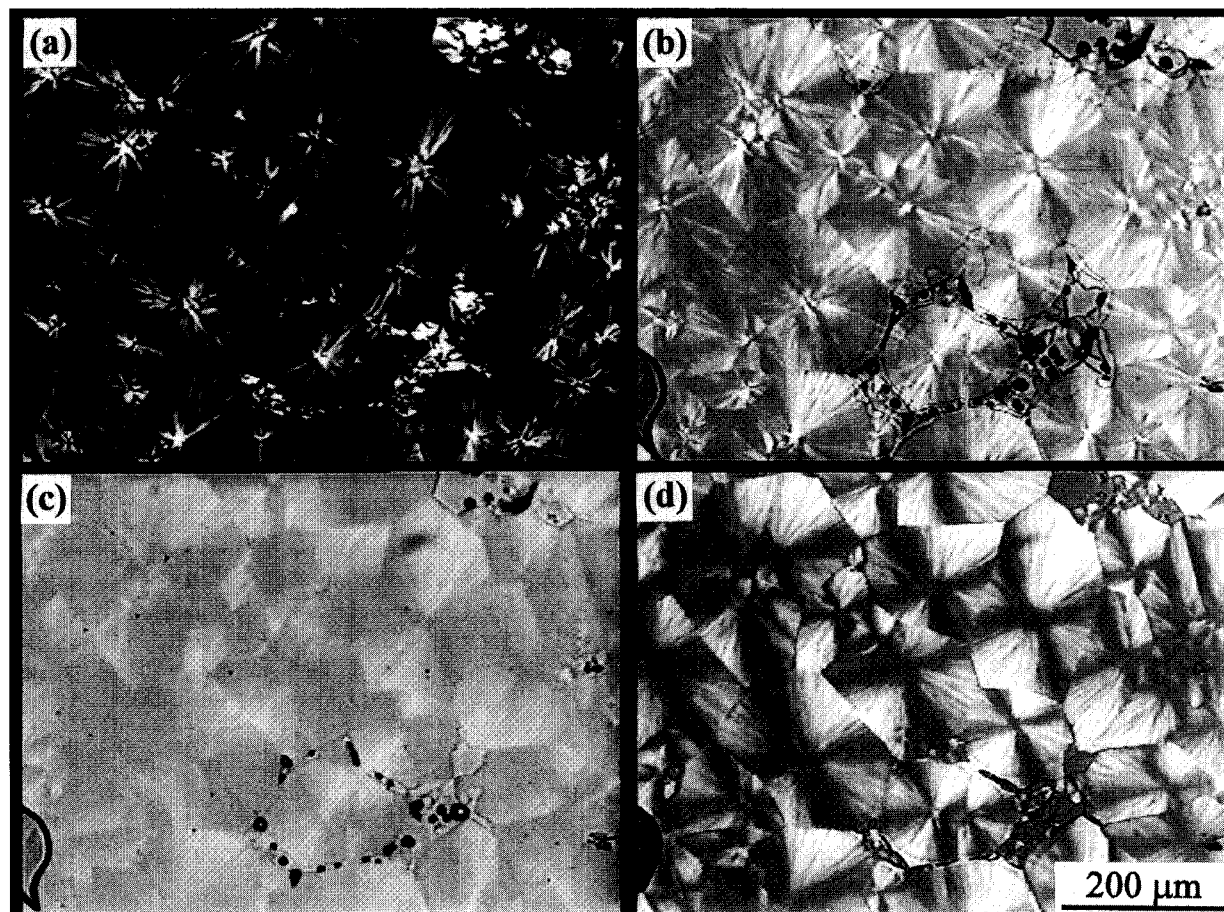
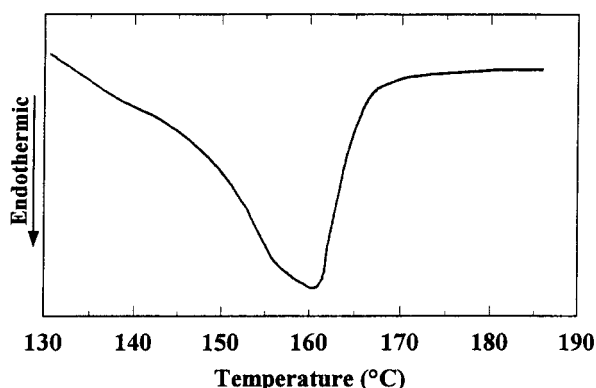


Figure 17 Polarized light microscopy of a PP sample exposed for 6 weeks. The specimen was crystallized at  $13^{\circ}\text{C min}^{-1}$  then heated rapidly to  $158^{\circ}\text{C}$  and kept at this temperature. (a) Initial morphology, before heating; (b) at  $152^{\circ}\text{C}$ ; (c) at  $158^{\circ}\text{C}$ , 0 min; (d) at  $158^{\circ}\text{C}$ , 5 min

enhanced by segregation effects<sup>57</sup>. Re-organization during heating, the other reason for peak duplication, presumably occurs only with samples crystallized at low temperatures, because unstable crystals are produced<sup>8</sup>.

The thermogram of *Figure 18* did not change when the cell was cooled to room temperature before the final melting, suggesting that no significant further crystallization occurred to alter the thermogram. In another example, a 12 weeks exposed sample was crystallized at 132.5°C and, after cooling to room temperature, the melting thermogram displayed a small peak with a maximum at ~131°C (*Figure 19a*). Since  $T_m < T_c$ , the crystals that yielded this peak were certainly produced during cooling prior to the final melting. From the crystallization exotherm of this sample (see *Figure 19b*),



**Figure 18** Melting thermogram (at 10°C min<sup>-1</sup>) of 6 weeks exposed PP crystallized at 130°C

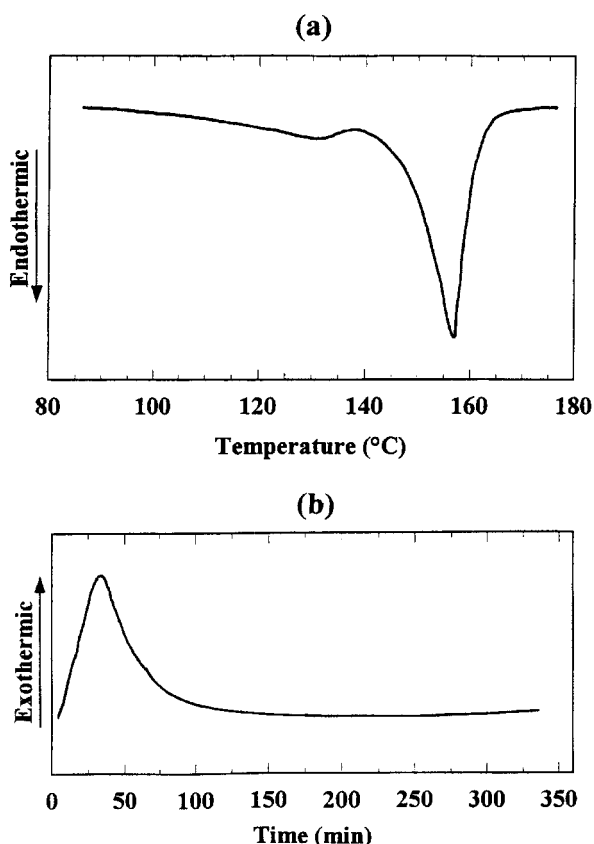


**Figure 19** (a) Melting thermogram (at 10°C min<sup>-1</sup>) of 12 weeks exposed PP crystallized at 132.5°C. (b) Exotherm during isothermal crystallization at 132.5°C

it appears that the crystallization was completed. The crystals that yielded the lower  $T_m$  were probably produced from molecules with much higher concentration of impurities than those which contributed to the main peak. These molecules showed negligible rates of crystallization at 132.5°C and the thermal output was too low to be detected by DSC.

## CONCLUSIONS

The crystallization behaviour of photo-degraded polypropylene has been followed after exposure times up to 48 weeks and the main conclusions are as follows.

- (1) Even after extensive chemical degradation, the ability of polypropylene to crystallize is preserved, but the presence of impurities in the molecules decreases the degree of crystallinity and the crystallization temperature during non-isothermal crystallization experiments. In many respects, the photo-degraded PP displays a crystallization behaviour similar to that of PP containing impurities, like in random copolymers;
- (2) The presence of defects and/or the low molecular weight caused the highly degraded materials to crystallize partially into the  $\gamma$ -phase;
- (3) At a constant crystallization temperature, the rate of crystallization decreased with exposure time (except for the sample exposed for 3 weeks), whilst at a constant supercooling the crystallization rate was much higher for degraded PP. These results were discussed based on the importance of molecular weight and chemical defects on the rates of nucleation and growth;
- (4) The isothermal crystallization of degraded polypropylene involves a two-stage process, possibly due to the segregation of molecules containing a large concentration of chemical impurities. This results in a decrease in the rate of spherulite growth at the later stage of crystallization, and in some cases a change in morphology along the spherulite radius was observed;
- (5) The melting thermograms showed double peaks which may have different causes. In samples crystallized non-isothermally from the melt, the peak duplication was shown to be caused by re-organisation during heating. Molecular segregation had little effect on this behaviour, but in samples crystallized isothermally the presence of different crystal populations was noted.

## ACKNOWLEDGEMENTS

The authors are grateful to ICI for providing the materials used in this investigation and to S.R. Holding of Rapra Technology Ltd for making the GPC measurements. MSR is grateful for a CAPES scholarship funded by the Brazilian government. The equipment in the artificial weathering laboratory was funded by grants from EPSRC.

## REFERENCES

1. Carlsson, D. J. and Wiles, D. M., *J. Macromol. Sci., Rev. Macromol. Chem.*, 1976, **C14**, 665.
2. Tribout, C., Monasse, B. and Haudin, J. M., *Colloid Polym. Sci.*, 1996, **274**, 197.
3. Martuscelli, E., Pracella, M. and Crispino, L., *Polymer*, 1983, **24**, 693.

4. Janimak, J. J., Cheng, S. Z.D., Giusti, P. A. and Hsieh, E. T., *Macromolecules*, 1991, **24**, 2253.
5. Janimak, J. J., Cheng, S. Z., Zhang, A. and Hsieh, E. T., *Polymer*, 1992, **33**, 728.
6. Monasse, B. and Haudin, J. M., *Colloid Polym. Sci.*, 1988, **266**, 679.
7. Wang, Y. F. and Lloyd, D. R., *Polymer*, 1993, **34**, 4740.
8. Varga, J., in *Polypropylene: Structure, Blends and Composites*, Vol.1, ed. J. Karger-Kocsis. Chapman and Hall, London, 1995, chap. 3, p.56.
9. Paukkeri, R. and Lehtinen, A., *Polymer*, 1993, **34**, 4083.
10. Kim, C. Y. and Kim, Y. C., *Polym. Eng. Sci.*, 1993, **33**, 1445.
11. Pospisil, L. and Rybnikar, F., *Polymer*, 1990, **31**, 476.
12. Pospisil, L., Jancar, J. and Rybnikar, F. J., *Mater. Sci. Lett.*, 1990, **9**, 495.
13. Wenxiu, C. and Shui, Y., *Radiat. Phys. Chem.*, 1993, **42**, 207.
14. Tiganis, B. E., Shanks, R. A. and Long, Y., *J. Appl. Polym. Sci.*, 1996, **59**, 663.
15. Rabello, M.S. and White, J.R., *Polymer*, 1997, **38**, 6379.
16. Hay, J.N., *Br. Polym. J.*, 1979, **11**, 37.
17. Wunderlich, B., *Macromolecular Physics*, Vol. 2: *Crystal Nucleation, Growth, Annealing*, Academic Press, New York, 1976.
18. Lauritzen, J. I. and Hoffman, J. D., *J. Res. Nat. Bur. Std.*, 1960, **64A**, 73.
19. Weidinger, A. and Hermans, P. H., *Makromol. Chem.*, 1961, **50**, 98.
20. Ogier, L., Rabello, M. S. and White, J. R., *J. Mater. Sci.*, 1995, **30**, 2364.
21. Addink, E. J. and Beintema, J., *Polymer*, 1961, **2**, 185.
22. Campbell, R. A., Phillips, P. J. and Lin, J. S., *Polymer*, 1993, **34**, 4809.
23. Meille, S. V., Ferro, D. R. and Bruckner, S., *Macromol. Symp.*, 1995, **89**, 499.
24. Turner-Jones, A., Aizlewood, J. M. and Beckett, D. R., *Makromol. Chem.*, 1964, **75**, 134.
25. Turner-Jones, A., *Polymer*, 1971, **12**, 487.
26. Schurz, J. M., Zipper, P. and Lenz, J., *J. Macromol. Sci., Pure Appl. Chem.*, 1993, **A30**, 603.
27. Kalay, G., Zhong, Z., Allan, P. and Bevis, M. J., *Polymer*, 1996, **37**, 2077.
28. Alamo, R. G., Galante, M. J., Lucas, J. C. and Madelkern, L., *Polym. Prepr.*, 1995, **36**, 285.
29. Avella, M., Erba, R., Martuscelli, E. and Ragosta, G., *Polymer*, 1993, **34**, 2951.
30. Vaughan, A. S. and Stevens, G. C., *Polymer*, 1995, **36**, 1531.
31. Schultz, J.M., *Polymer Materials Science*. Prentice-Hall, New Jersey, 1974.
32. Wunderlich, B., *Macromolecular Physics. Vol.3. Crystal Melting*. Academic Press, New York, 1980.
33. Mezghani, K., Campbell, R. A. and Phillips, P. J., *Macromolecules*, 1994, **27**, 997.
34. Keith, H. D. and Padden, F. J., *J. Appl. Phys.*, 1964, **35**, 1286.
35. Phillips, P.J., in *Crystallization of Polymers*, Ed. M.Dosiere. Kluwer Academic Publishers, Dordrecht, 1993, p.301.
36. Bassett, D.C., *Principles of Polymer Morphology*. Cambridge University Press, Cambridge, 1981.
37. Calvert, P. D. and Ryan, T. G., *Polymer*, 1984, **25**, 921.
38. Keith, H. D. and Padden, F. J., *J. Appl. Phys.*, 1964, **35**, 1270.
39. Gedde, U. W. and Jansson, J. F., *Polymer*, 1984, **25**, 1263.
40. Keith, H. D. and Padden, F. J., *J. Appl. Phys.*, 1963, **34**, 2409.
41. Bassett, D. C. and Vaughan, A. S., *Polymer*, 1986, **27**, 1472.
42. Kamide, K. and Yamaguchi, K., *Makromol. Chem.*, 1972, **162**, 219.
43. Shi, G., Zhang, X., Cao, Y. and Hong, J., *Makromol. Chem.*, 1993, **194**, 269.
44. Rybnikar, F. J., *Macromol. Sci. Phys.*, 1991, **B30**, 201.
45. O'Kane, W. J., Young, R. J., Ryan, A. J., Bras, W., Derbyshire, G. E. and Mant, G. R., *Polymer*, 1994, **35**, 1352.
46. Guerra, G., Petraccone, V., Corradini, P., Rosa, C., Napolitano, R., Pirozzi, B. and Giunchi, G. J., *Polym. Sci. Polym. Phys. Edn.*, 1984, **22**, 1029.
47. Duvall, J., Selliti, C., Myers, C., Hiltner, A. and Baer, E., *J. Appl. Polym. Sci.*, 1994, **52**, 207.
48. Cox, W. W. and Duswalt, A. A., *Polym. Eng. Sci.*, 1967, **7**, 309.
49. Yoshii, F., Meligi, G., Sasaki, T., Makuuchi, K., Rabi, A. M. and Nishimoto, S., *Polym. Degrad. Stab.*, 1995, **49**, 315.
50. Horrocks, A. R., Valinejad, K. and Crighton, J. S., *J. Appl. Polym. Sci.*, 1994, **54**, 593.
51. Busfield, W. K. and O'Donnell, J. H., *Eur. Polym. J.*, 1979, **15**, 197.
52. Allen, N. S., Edge, M., Corrales, T., Shah, M., Holdsworth, D., Catalina, F., Peinado, C. and Collar, E. P., *Polymer*, 1996, **37**, 2323.
53. Puig, C. C., Odell, J. A., Hill, M. J., Barham, P. J. and Folkes, M. J., *Polymer*, 1994, **35**, 2452.
54. Rabello, M.S. PhD Thesis, University of Newcastle upon Tyne, 1996.
55. Padden, F. J. and Keith, H. D., *J. Appl. Phys.*, 1959, **30**, 1479.
56. Norton, D. R. and Keller, A., *Polymer*, 1985, **26**, 704.
57. Yadav, Y. S. and Jain, P. C., *Polymer*, 1986, **27**, 721.